ADVANCED ENERGY MATERIALS

Supporting Information

for *Adv. Energy Mater.*, DOI 10.1002/aenm.202300574

3D Macroporous Frame Based Microbattery With Ultrahigh Capacity, Energy Density, and Integrability

*Wei Yang, Lin Xu, Wen Luo, Ming Li, Ping Hu, Yuhang Dai, Fazhi Ye, Chunhua Han, Minxuan Zhou, Rong Tu, Ji Shi and Liqiang Mai**

Supporting Information

3D macroporous frame based microbattery with ultrahigh capacity, energy density, and integrability

Wei Yang, Lin Xu, Wen Luo, Ming Li, Ping Hu, Yuhang Dai, Fazhi Ye, Chunhua Han, Minxuan Zhou, Rong Tu, Ji Shi, Liqiang Mai*

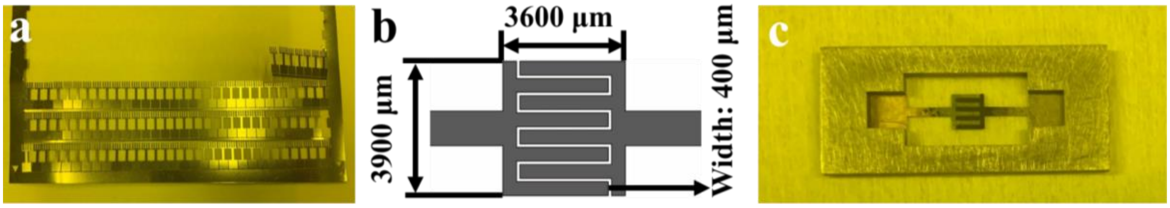

Figure S1. (a) Digital image of patterned Ni microelectrodes fabricated by commercial large-scale wet etching (Fabricated by Shaoxing Hua Li Electronics Co., Ltd, the thickness of raw Ni foil is 100 μm). (b) The projection shows the design of the microelectrodes. (c) Fabrication process under assembly tool.

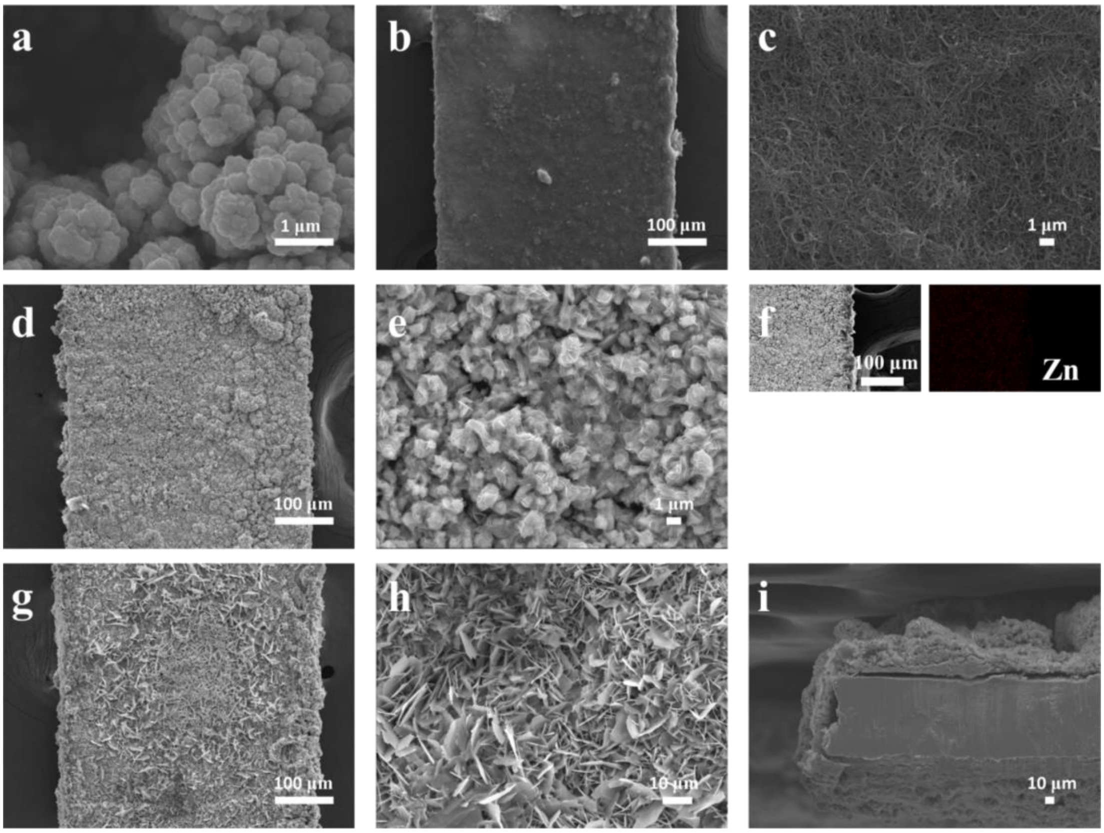

Figure S2. SEM image of (a) 3D macroporous Ni microelectrode, (b, c) CNT-coated brass microelectrode, (d, e) Zn@CNT brass microelectrode. (f) EDS mapping images of the edge side of Zn@CNT brass microelectrode. (g, h) The surface and (i) the cross-section of Zn@CNT brass microelectrode after cycling.

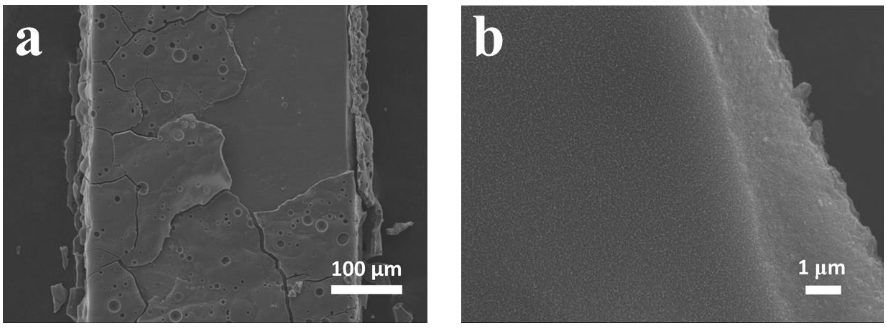

Figure S3. SEM images of PEDOT-MnO_2-70 film on a planar microelectrode.

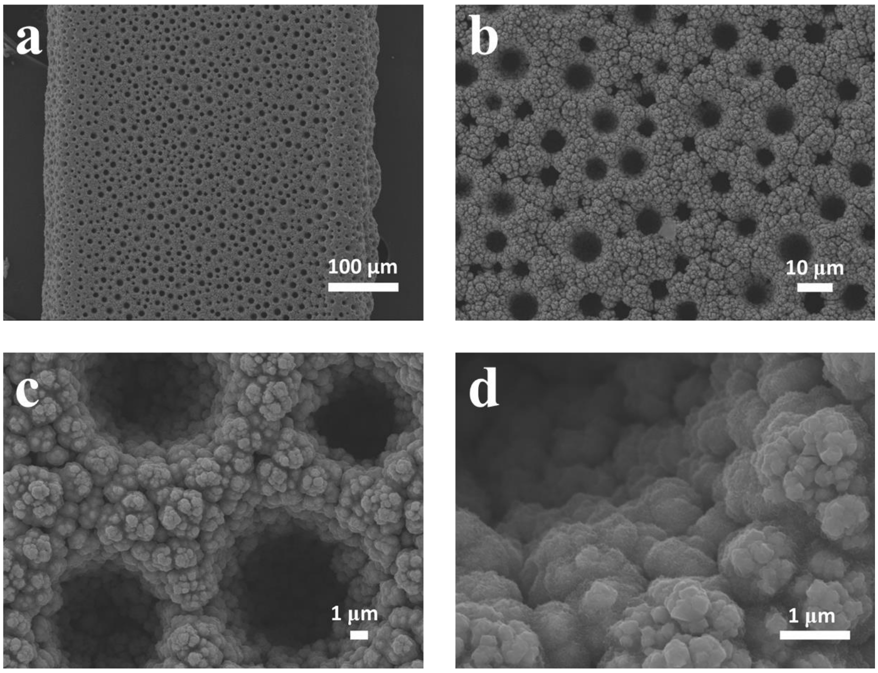

Figure S4. SEM images of PEDOT-MnO_2-10 microelectrode.

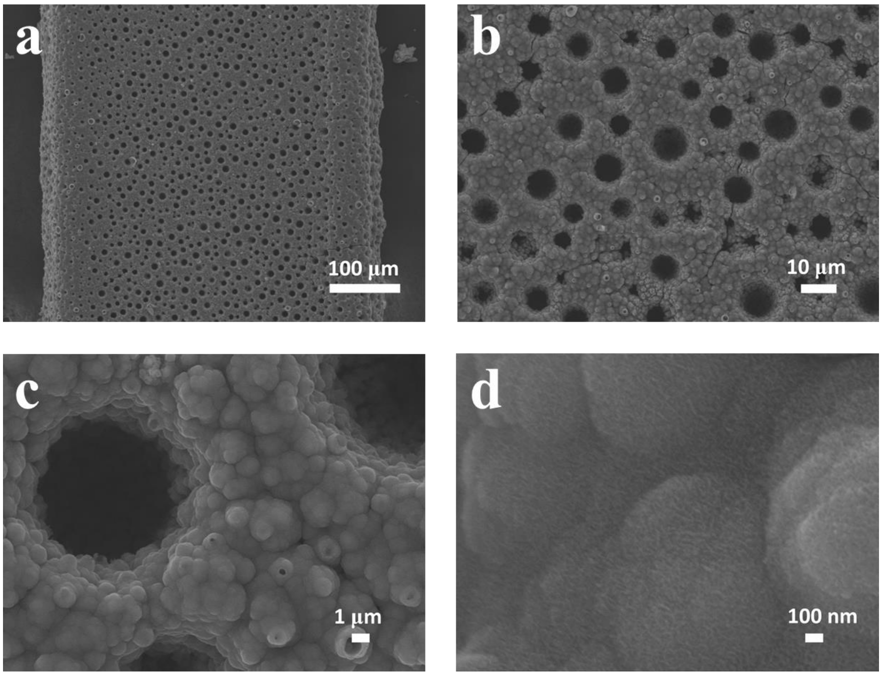

Figure S5. SEM images of PEDOT-MnO_2-30 microelectrode.

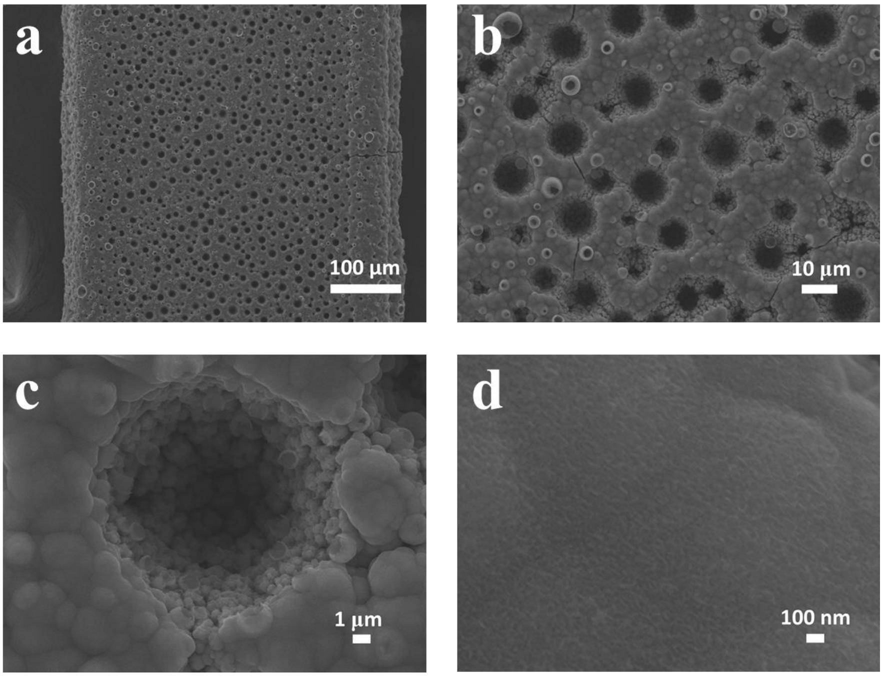

Figure S6. SEM images of PEDOT-MnO_2-50 microelectrode.

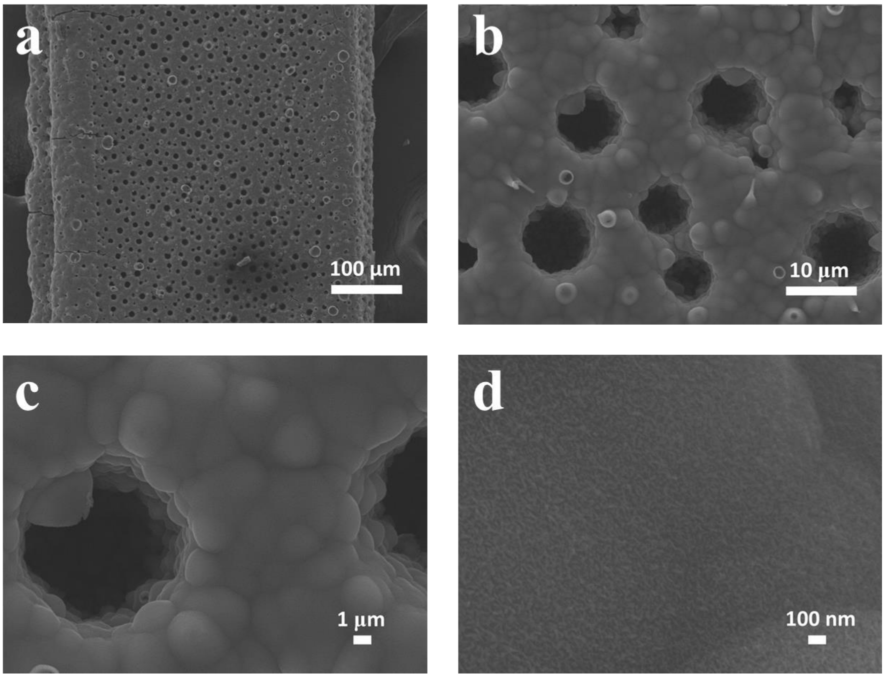

Figure S7. SEM images of PEDOT-MnO_2-70 microelectrode.

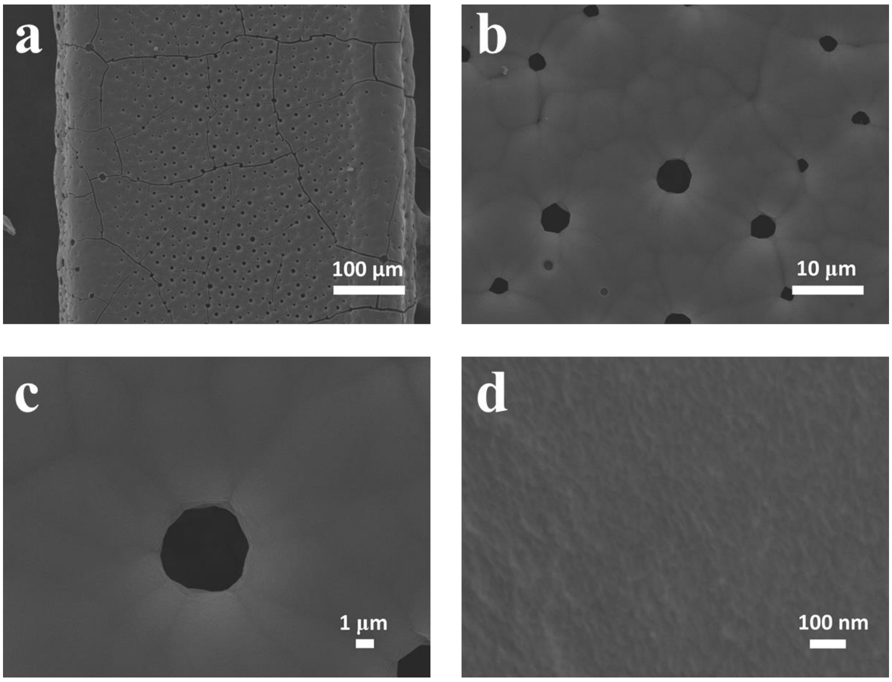

Figure S8. SEM images of PEDOT-MnO_2-90 microelectrode.

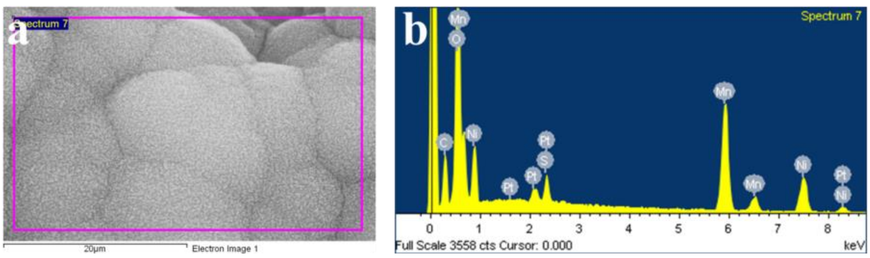

c

Element	Atomic%
C K	27.40
O K	52.67
S K	1.17
Mn K	11.24
Ni K	7.24
Pt M	0.29

Figure S9. EDS spectrum of PEDOT-MnO_2-70 microelectrode.

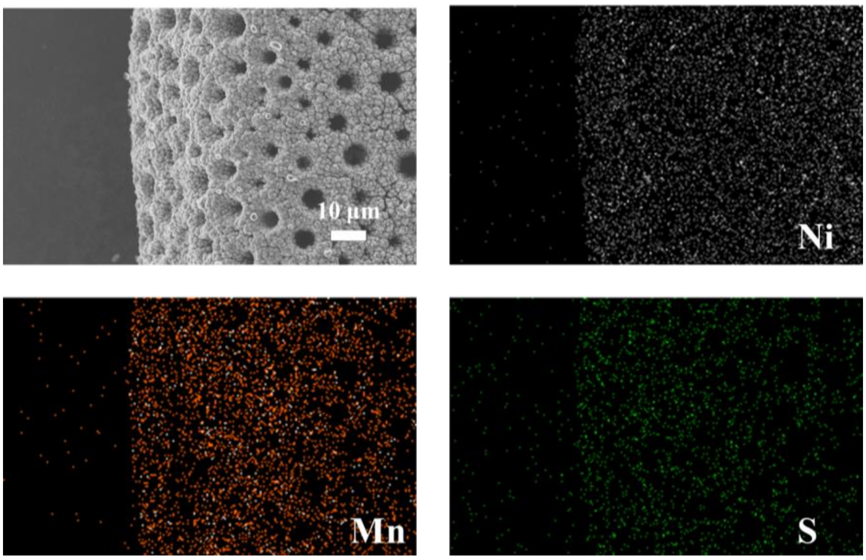

Figure S10. SEM and EDS mapping images of the edge side of PEDOT-MnO_2-10 microelectrode.

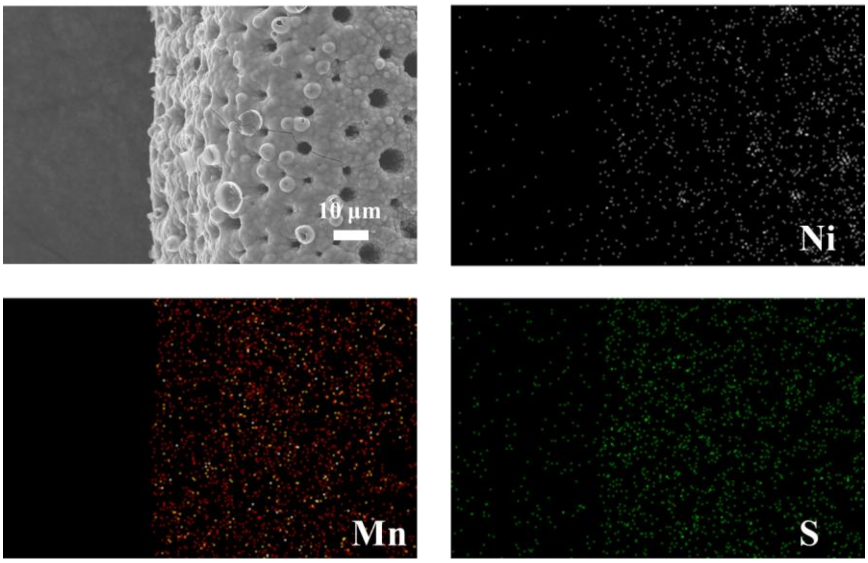

Figure S11. SEM and EDS mapping images of the edge side of PEDOT-MnO_2-30 microelectrode.

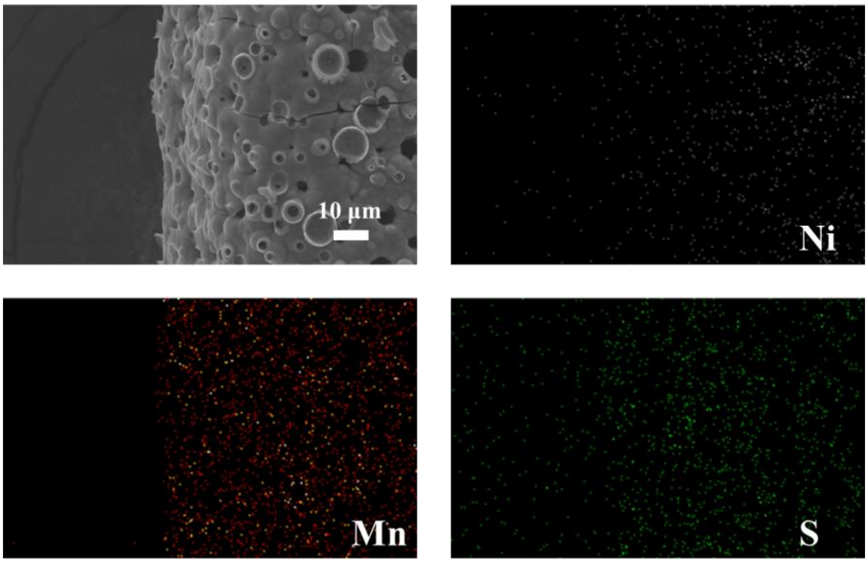

Figure S12. SEM and EDS mapping images of the edge side of PEDOT-MnO_2-50 microelectrode.

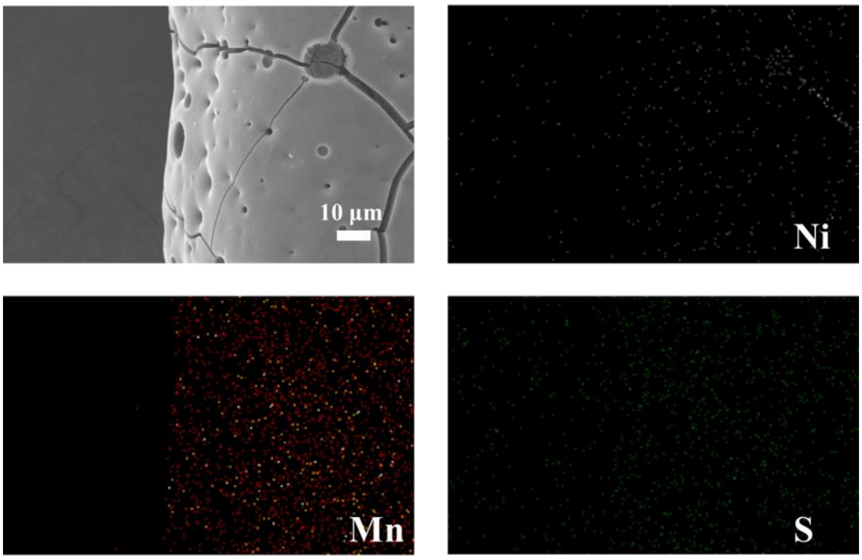

Figure S13. SEM and EDS mapping images of the edge side of PEDOT-MnO_2-90 microelectrode.

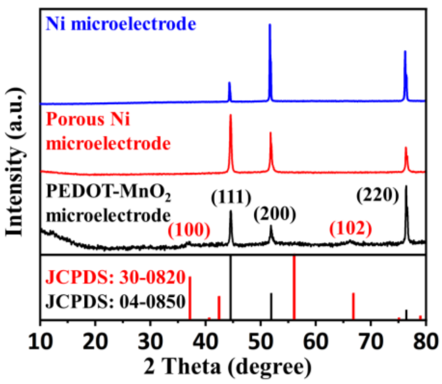

Figure S14. XRD patterns of Ni, porous Ni and PEDOT-MnO_2-70 microelectrodes.

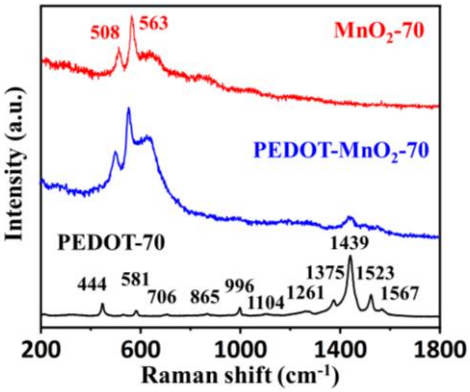

Figure S15. Raman spectrum of MnO_2-70, PEDOT-MnO_2-70, and PEDOT-70 microelectrodes.

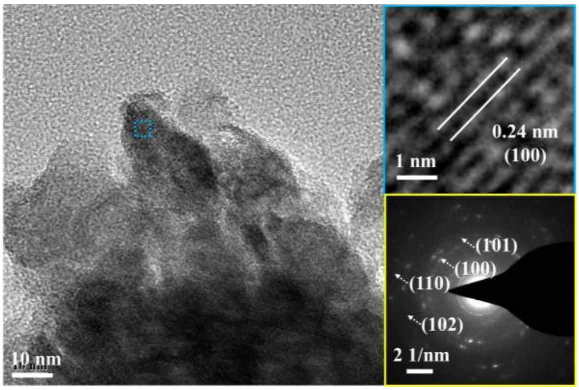

Figure S16. HRTEM and SAED images of PEDOT-MnO_2-70.

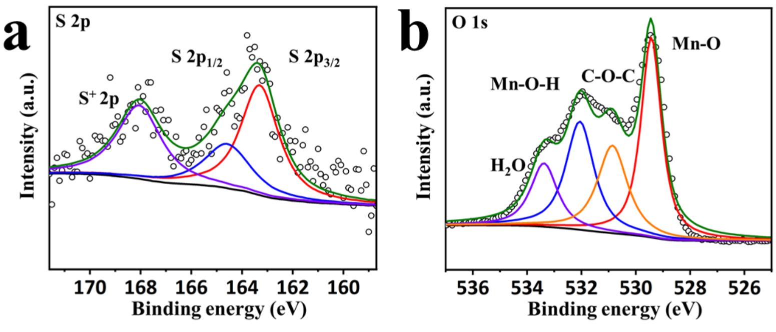

Figure S17. XPS spectra of (a) S 2p and (b) O 1s of PEDOT-MnO_2-70 microelectrodes.

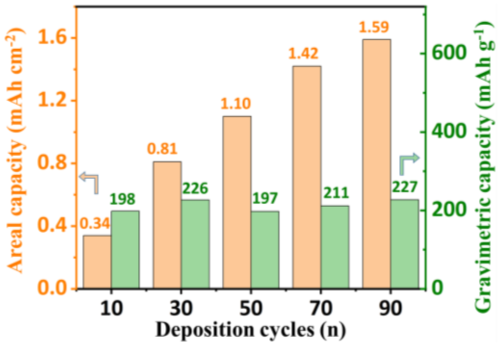

Figure S18. Gravimetric capacity is based on the mass of active materials at the current density of 1 mA cm^{-2}.

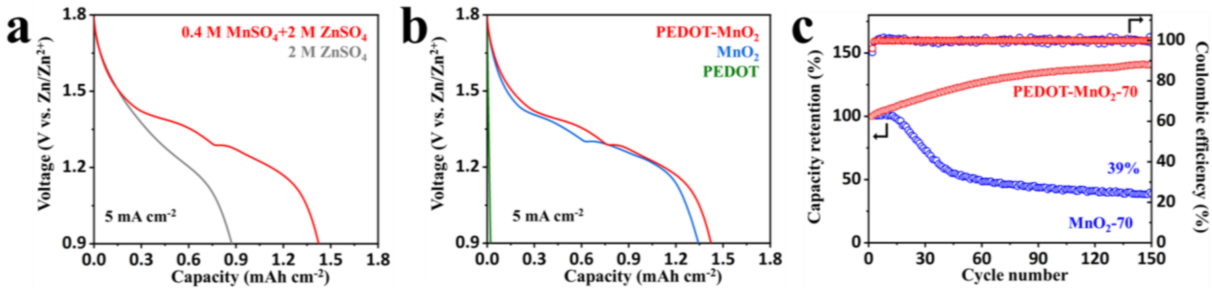

Figure S19. (a) Areal capacity of PEDOT-MnO_2-70 with or without Mn^{2+} additive. (b) Areal capacity of PEDOT-MnO_2-70, PEDOT-70 and MnO_2-70. (c) Cycling performance and Coulombic efficiency of MnO_2-70 and PEDOT-MnO_2-70 microelectrodes.

The reaction mechanism of the Zn-Mn MB could be explained as the insertion/extraction of Zn^{2+} and H^+ and dissolution/deposition of Mn^{2+}. The reaction process can be described below

Cathode:

$MnO_2 + 4H^+ + 2e^- \leftrightarrow Mn^{2+} + 2H_2O$

$MnO_2 + H^+ + e^- \leftrightarrow MnOOH$

$2MnO_2 + Zn^{2+} + 2e^- \leftrightarrow ZnMn_2O_4$

Anode:

$Zn^{2+} + 2e^- \leftrightarrow Zn$

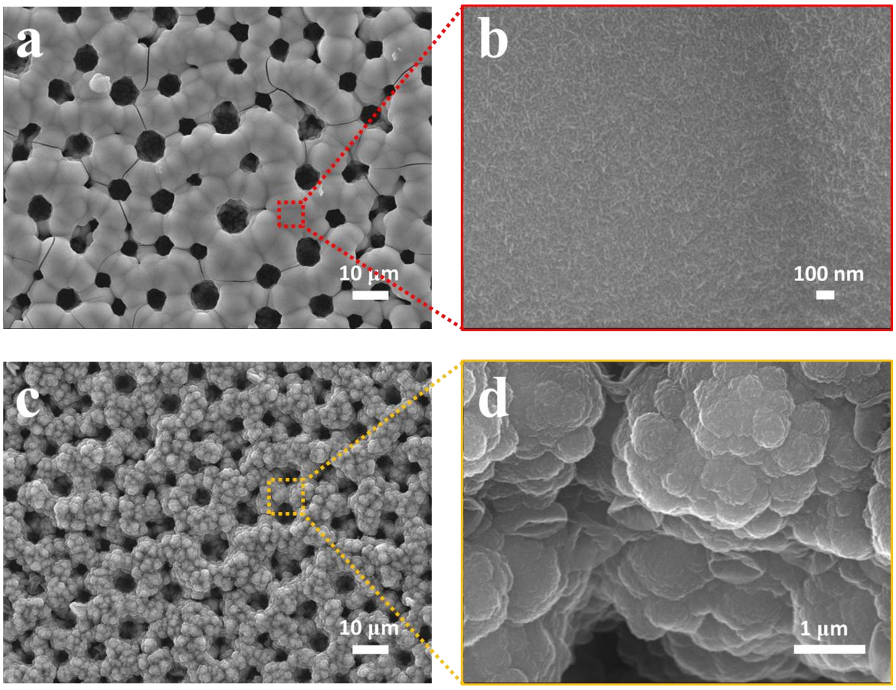

Figure S20. SEM images of (a, b) MnO_2-70 and (c, d) PEDOT-70 microelectrodes.

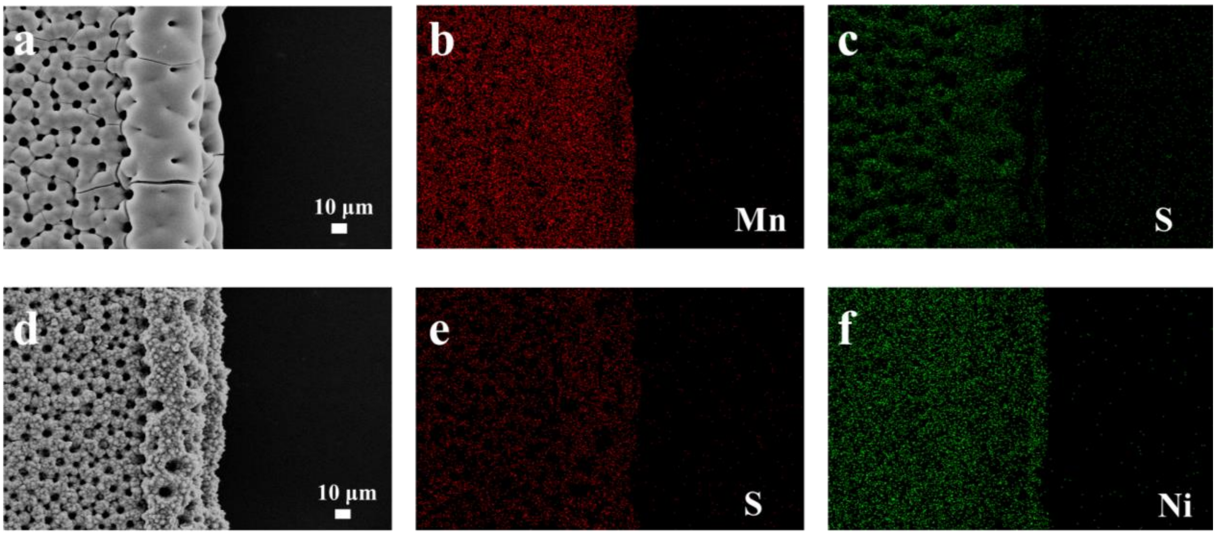

Figure S21. SEM and EDS mapping images of the edge side of (a-c) MnO_2-70 and (d-f) PEDOT-70 microelectrode.

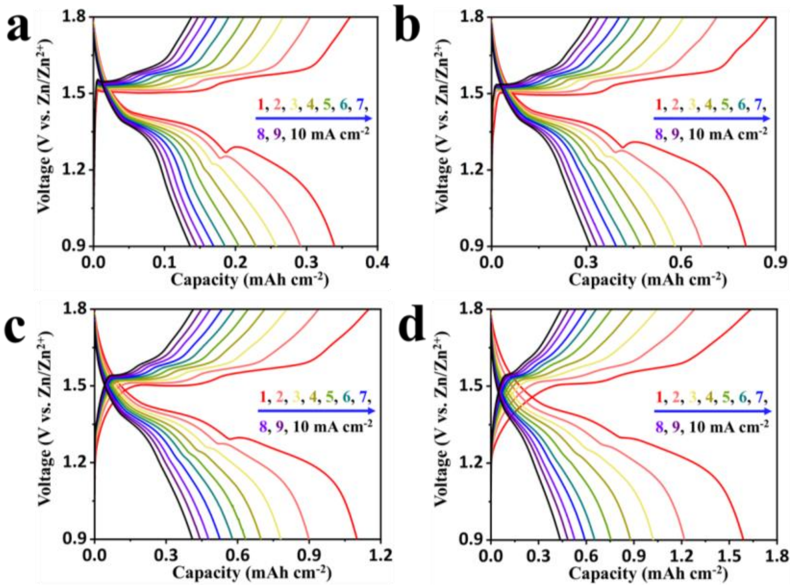

Figure S22. GCD curves of PEDOT-MnO_2-10, 30, 50, and 90 at various current densities ranging from 1 to 10 mA cm^{-2}.

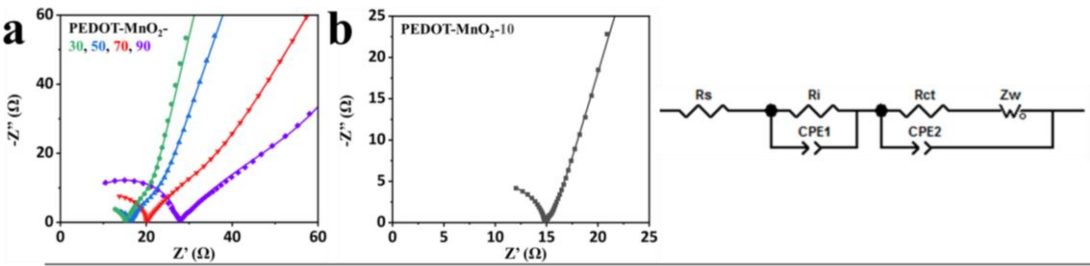

c

PEDOT-MnO_2-	10	30	50	70	90
R_s (Ω)	3.3	3.1	3.1	3.1	3.2
R_i (Ω)	11.5	12.2	13.0	16.9	24.0
R_{ct} (Ω)	0.2	24.6	27.0	41.0	141.7

Figure S23. EIS of PEDOT-MnO_2-10 to 90.

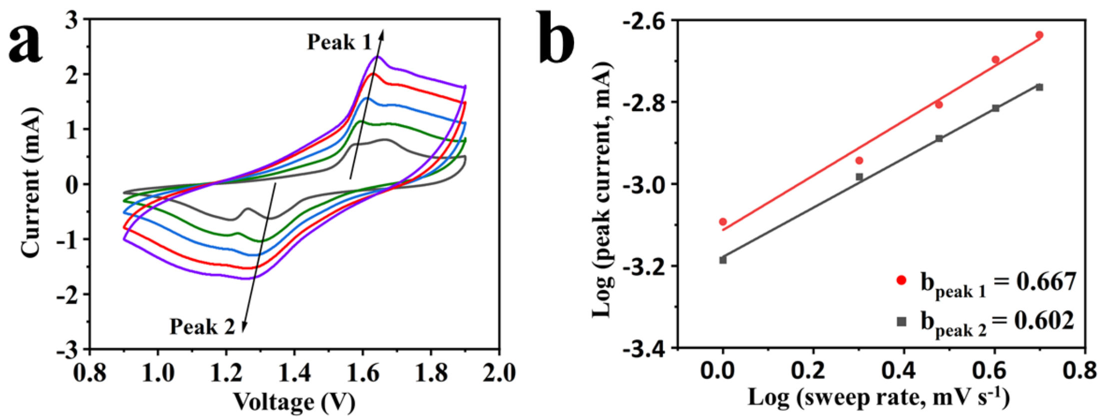

Figure S24. (a) CV curves from 1 to 5 mV s^{-1}. (b) The fitting lines between log(i) and log(v) at specific peak currents from CV curves.

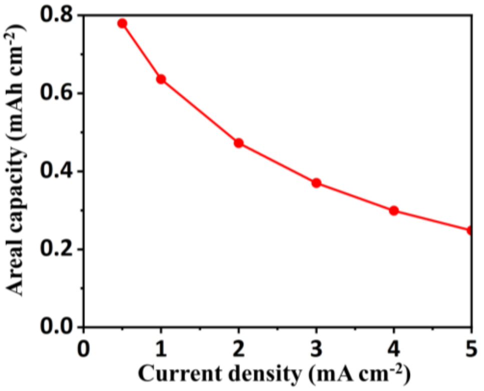

Figure S25. The areal capacities of PEDOT-MnO_2-70 at various current densities.

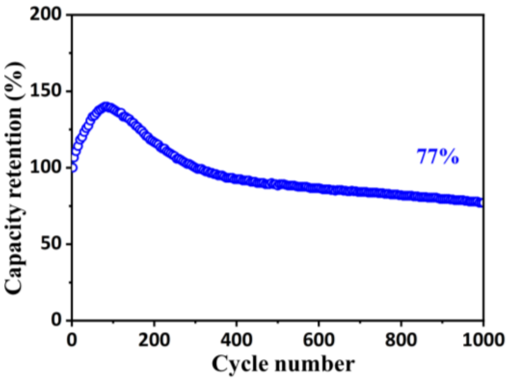

Figure S26. The capacity retention of PEDOT-MnO_2//Zn MB.

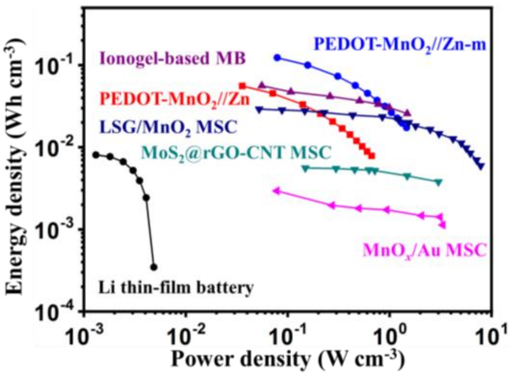

Figure S27. Ragone plots showing the volumetric energy/power densities of our work and other MESDs.

The PEDOT-MnO_2//Zn (PEDOT-MnO_2//Zn-m) MB delivers high volumetric energy densities of 53 mWh cm^{-3} (117 mWh cm^{-3}) at a current density of 0.1 mA cm^{-2}, which exceeds many reported MESDs, about 55.6 mWh cm^{-3} for Ionogel-based MB,[S1] 29 mWh cm^{-3} for LSG/MnO_2 MSC,[S2] 5.6 mWh cm^{-3} for MoS_2@rGO-CNT MSC,[S3] and 1.75 mWh cm^{-3} for MnO_x/Au MSC.[S4]

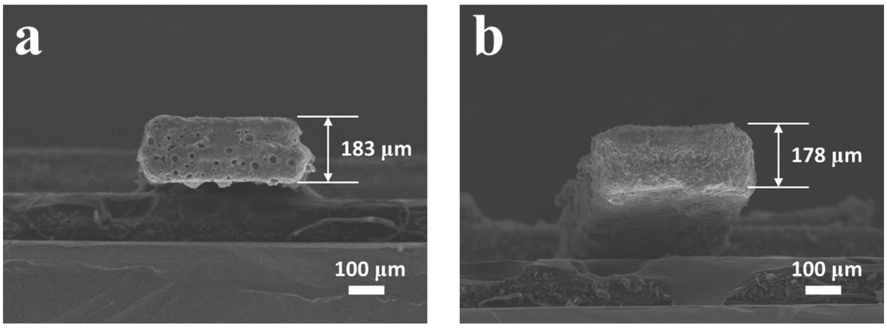

Figure S28. The cross-section SEM images of (a) PEDOT-MnO_2-70 and (b) Zn@CNT microelectrodes.

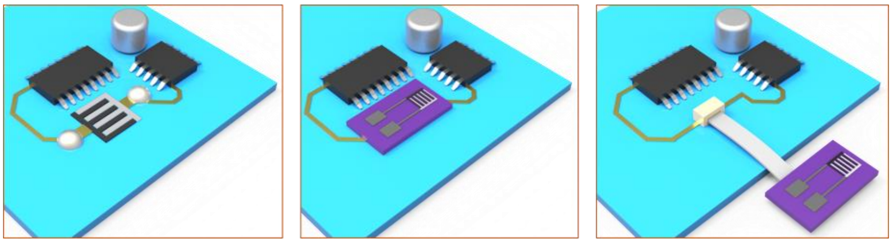

Figure S29. Comparison of integration methods of MBs with substrate-free and bottom-up microelectrodes.

The MESD with substrate-free microelectrodes can be embedded in the circuit board directly. Nevertheless, the "bottom-up" MESD commonly integrate with other compounds by transferring the whole device to another substrate.[S5] Otherwise, an external line should connect the PCB and the MESD.[S6]

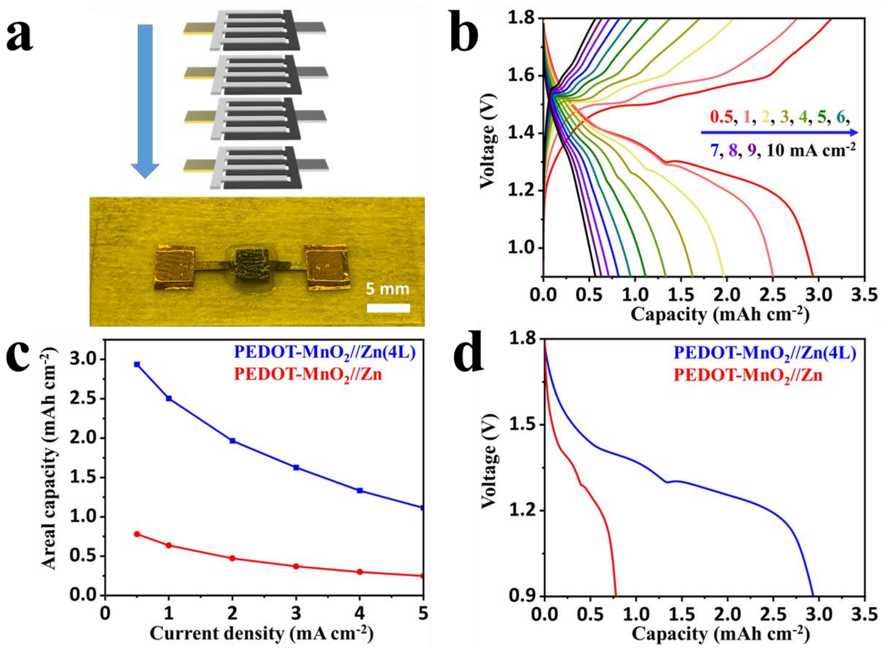

Figure S30. (a) Digital image of PEDOT-MnO_2//Zn(4L) MB. (b) GCD curves of PEDOT-MnO_2//Zn(4L) MB. (c) Rate capability and (d) GCD curves at 0.5 mA cm^{-2} of PEDOT-MnO_2//Zn and PEDOT-MnO_2//Zn(4L) MBs.

Table 1. Comparison of areal capacity (capacitance) and maximum areal energy/power densities between our MB with other previously reported MnO_2 and PEDOT based MESDs.

MESDs	Areal capacity/capacitance	Maximum areal energy density	Maximum areal power density	Ref.
3D NCA-engineered Zn−Mn MB	0.436 mAh cm^{-2} @ 0.06 mA cm^{-2}	N/A	N/A	S7
3D hybrid asymmetric MSC	665.3 mF cm^{-2} @ 3.2 mA cm^{-2}	182.3 μWh cm^{-2}	33.9 mW cm^{-2}	S8
Ni@MnO_2//Zn MB	0.718 mAh cm^{-2} @ 0.1 mA cm^{-2}	0.98 mWh cm^{-2}	1.3 mW cm^{-2}	S9
Na-MnO_x@NCF//VN NSAs MSC	109.5 mF cm^{-2} @ 1 mA cm^{-2}	87.62 μWh cm^{-2}	12.1 mW cm^{-2}	S10
3D PEDOT//Fe_2O_3 MSC	21.3 mF cm^{-2}	N/A	N/A	S11
MnHCF-MnOx-Based MSC	16.8 mF cm^{-2}	2.3 μWh cm^{-2}	0.5 mW cm^{-2}	S12
3D printed MXene-AgNW-MnONW-C60 MSC	216.2 mF cm^{-2} @ 10 mV s^{-1}	19.2 μWh cm^{-2}	58.3 mW cm^{-2}	S13
MnO_2@Ppy@MWCNT MSC	21.8 mF cm^{-2} @ 0.1 mA cm^{-2}	12.16 μWh cm^{-2}	1.8 mW cm^{-2}	S14
ZIDMB	1.93 mAh cm^{-2} @ 2 mA cm^{-2}	2.34 mWh cm^{-2}	11.2 mW cm^{-2}	S15
Zn-Br_2 MB	2.2 mAh cm^{-2} @ 2 mA cm^{-2}	3.6 mWh cm^{-2}	26.2 mW cm^{-2}	S16
NVPF‖NaBF4-IE‖NTP NIMB/EC-8L	4.5 mAh cm^{-2} @ 2 mA cm^{-2}	7.33 mWh cm^{-2}	7.17 mW cm^{-2}	S17

PEDOT-MnO_2-70//Zn MB	0.78 mAh cm^{-2} @ 0.5 mA cm^{-2}	1.02 mWh cm^{-2}	12.16 mW cm^{-2}	This work
PEDOT-MnO_2-70//Zn(4L) MB	2.94 mAh cm^{-2} @ 0.5 mA cm^{-2}	3.87 mWh cm^{-2}	12.77 mW cm^{-2}	This work

References

[S1] S. Zheng, H. Huang, Y. Dong, S. Wang, F. Zhou, J. Qin, C. Sun, Y. Yu, Z.-S. Wu, X. Bao, *Energy Environ. Sci.* **2020**, 13, 821-829.

[S2] M. F. El-Kadya, M. Ihnsa, M. Lia, J. Y. Hwanga, M. F. Mousavia, L. Chaneya, A. T. Lecha, R. B. Kanera, *Proc. Natl. Acad. Sci. USA* **2015**, 112, 4233-4238.

[S3] W. Yang, L. He, X. Tian, M. Yan, H. Yuan, X. Liao, J. Meng, Z. Hao, L. Mai, *Small* **2017**, 1700639.

[S4] W. Si, C. Yan, Y. Chen, S. Oswald, L. Hana, O. G. Schmidt, *Energy Environ. Sci.* **2013**, 6, 3218-3223.

[S5] Y. Yue, Z. Yang, N. Liu, W. Liu, H. Zhang, Y. Ma, C. Yang, J. Su, L. Li, F. Long, Z. Zou, Y. Gao, *ACS Nano* **2016**, 10, 11249-11257.

[S6] J. Liang, B. Tian, S. Li, C. Jiang, W. Wu, *Adv. Energy Mater.* **2020**, 2000022.

[S7] H. Liu, G. Zhang, L. Wang, X. Zhang, Z. Zhao, F. Chen, L. Song, H. Duan, *ACS Appl. Energy Mater*. **2021**, 4, 10414−10422.

[S8] F. Li, M. Huang, J. Wang, J. Qu, Y. Li, L. Liu, V. K. Bandari, Y. Hong, B. Sun, M. Zhu, F. Zhu, Y. X. Zhang, O. G. Schmidt, *Energy Storage Materials* **2020**, 27, 17–24.

[S9] B. He, Q. Zhang, L. Li, J. Sun, P. Man, Z. Zhou, Q. Li, J. Guo, L. Xie, C. Li, X. Wang, J. Zhao, T. Zhang, Y. Yao, *J. Mater. Chem. A* **2018**, 6, 14594-14601.

[S10] Q. Zhang, J. Zhang, Z. Zhou, L. Wei, Y. Yao, *J. Mater. Chem. A*, 2018, 6, 20145.

[S11] Y. Diao, Y. Lu, H. Yang, H. Wang, H. Chen, J. M. D'Arcy, *Adv. Funct. Mater.* **2020**, 2003394.

[S12] J. Liang, B. Tian, S. Li, C. Jiang, W. Wu, *Adv. Energy Mater.* **2020**, 2000022.

[S13] X. Li, H. Li, X. Fan, X. Shi, J. Liang, *Adv. Energy Mater.* **2020**, 1903794.

[S14] J. Gao, C. Shao, S. Shao, F. Wan, C. Gao, Y. Zhao, L. Jiang, L. Qu, *Small*, **2018**, 14, 1801809.

[S15] X. Jin, L. Song, C. Dai, Y. Xiao, Y. Han, X. Li, Y. Wang, J. Zhang, Y. Zhao, Z. Zhang, N. Chen, L. Jiang, L. Qu, *Adv. Mater.* **2022**, 2109450.

[S16] C. Dai, L. Hu, X. Jin, Y. Wang, R. Wang, Y. Xiao, X. Li, X. Zhang, L. Song, Y. Han, H. Cheng, Y. Zhao, Z. Zhang, F. Liu, L. Jiang, L. Qu, *Sci. Adv.* **2022**, 8, eabo6688.

[S17] J. Ma, S. Zheng, L. Chi, Y. Liu, Y. Zhang, K. Wang, Z.-S. Wu, *Adv. Mater.* **2022**, 34, 2205569.